

# Ground motion relations for India

## Abstract

In this article, a study on attenuation of ground motion is undertaken for India. To derive the relations, India is divided into seven regions based on seismo-tectonic setting and geology. Due to lack of strong motion data, finite source seismological model is used for generating synthetic database. The input parameters in the seismological model are taken specific to the region. Uncertainty in the model parameters is considered. With the help of large synthetic database, ground motion relations for 5 % damped spectral acceleration are obtained by regression analysis. The developed ground motion relations are useful in preparing spectral acceleration hazard maps of India for a given annual probability of exceedance.

**Keywords :** Response spectra, Seismic hazard, Seismological model.

## 1. Introduction

Ground motion relation is a key component in probabilistic seismic hazard analysis (PSHA). Past experience shows that a site vibrates due to earthquakes originating anywhere in a region of about 300 km radius around the site. Thus regional properties and their local details play major roles in dictating the future seismic hazard at the site. In this context, ground motion relations have an important role in practical problems. These relations describes the average or other moments of the random hazard parameter in terms of magnitude and distance. Due to their importance, a number of ground motion relations for various parts of the world have been developed (Douglas 2003). Ideally one requires recorded strong motion data for all magnitudes in the range 4 to 8.5 and all distances in the range 0–300 km for developing ground motion relations. No tectonic region in India satisfy this demand on the database and therefore, a reliable assessment of ground motion attenuation is very difficult. Thus, considerable care is necessary in using attenuation relations which have been obtained with low magnitude earthquake data. Proposals to adopt equations from other regions of the world to Indian sites based on arguments of similarity are essentially intuitive in nature, lacking objectively verifiable rationale. For regions with very few strong motion data, it is more scientific to use the stochastic seismological model (Boore 1983) for generating large samples of artificial ground motion time histories. With the help of such a sample where in the uncertain source, path and site parameters can be randomly varied, one can arrive at reliable ground motion relations valid for a wider range of magnitude and hypocentral distance values. However, such a model needs to be validated with the help of some instrumental data. Since the subcontinent is too much varied in its geological structure a single equation to

cover all the land mass is unacceptable. This compels one to derive ground motion relations for important geological provinces in India differentiated in terms of their quality factors, and probable range of stress drop during future earthquakes. Validation of these equations is possible by comparing their predictions with actual recorded past strong motion data. This approach of deriving empirical attenuation relations through large scale computer simulation of synthetic accelerograms, has been previously used by Iyengar and Raghukanth (2004) and Raghukanth and Iyengar (2007). The major limitation of this effort was the point source assumption and hence it was unable to predict ground motion at sites near the faults. However the stochastic source mechanism model (Boore 1983, Boore 2009) can be improved to include sources of finite dimension. Stochastic seismological model for simulation of ground motion depends on region specific earthquake model parameters such as stress drop, slip distribution, dip of the fault plane, focal depth, site amplification function and the quality factor. These model parameters are available for India. This helps in fixation of the limit of uncertainties in the input parameters for India. With the help of large synthetic database, attenuation relations for 5 % damped Spectral acceleration are obtained by regression analysis. The derived ground motion relations are valid for A-type rock site which has its average shear wave velocity in the top thirty meters to be greater than 1.5 km/s.

## **2. Strong motion database**

Since earthquakes are quite common in Himalayas and in NEI, in 1985 three strong-motion arrays comprising of 135 stations were established in these regions (Chandrasekaran and Das 1992). The Kangra array is in the Himachal Pradesh region, the Shillong array is in NEI, and the Uttarakhand array is in northwest Himalayas. These arrays have recorded twenty-one individual earthquakes, with magnitudes lying between 4.5 and 7.2, recording 156 three component accelerograms. The strong-motion data for all these events are available in the global data base (<http://db.cosmos-eq.org/>). Out of the recorded earthquakes, seven occurred in Northeast India and remaining triggered in the Himalayas. Among the seven in northeast India, four events occurred in Indo-Burma ranges are related to subduction tectonics where as remaining three earthquakes are of crustal nature. A brief review of SMA data in Indian shield region is available in the article of Iyengar and Raghukanth (2004). Openly available SMA data of India is shown Figure 1 as a function of magnitude and hypocentral distance. It is observed that even if we take the whole country as a homogenous unit the SMA database is seriously deficient in all magnitude and distance ranges. Another major limitation with instrumental data in India is that, the nature of site of the recording station is not known. Hence any empirical attenuation relation proposed purely on past data can not be used as a credible tool in hazard estimation.

### 3. Finite source seismological model

Due to unavailability of strong motion records of past earthquakes, ground motions are simulated by an analytical model. The stochastic finite fault approach of Boore (2009) which is an improved version of the methodology proposed by Motazedian and Atkinson (2005) is used to simulate the rock level ground motion for the seven geological regions in India. The theory and application of seismological models for estimating ground motion has been discussed in detail by Boore (2009). The application of seismological model for estimating ground motion in northeastern India has been discussed in detail by Raghukanth and Somala (2009) and Raghukanth and Dash (2009). A brief description of the method starting with the frequency domain representation of the ground acceleration will bring out the advantages of this approach. In this method, the rectangular fault plane is divided into  $N$  number of subfaults and each subfault is represented as a point source. The Fourier amplitude spectrum of ground motion  $[A(r,f)]$  due to the  $j^{\text{th}}$  subfault at a site is derived from the point source seismological model, expressed as

$$A_j(r, f) = CH_j S_j(f) F(f) D(r, f) P(f) \quad (1)$$

Here  $C$  is a scaling factor,  $S_j(f)$  is the source spectral function,  $D(r,f)$  is the diminution function characterizing the quality of the region,  $P(f)$  is a filter function,  $F(f)$  is the site dependent function that modifies the bed rock motion in the vertical direction and  $H_j$  is a scaling factor used for conserving the energy of high-frequency spectral level of sub-faults. In the present study, following Brune (1970), the principal source model  $S_j(f)$  is taken

$$S_j(f) = (2\pi f)^2 \frac{M_{0j}}{\left[1 + \left(f/f_{0j}\right)^2\right]} \quad (2)$$

Here  $f_{0j}$  is the corner frequency and  $M_{0j}$  is the seismic moment of the  $j^{\text{th}}$  subfault. The three important seismic source parameters  $M_0$ ,  $f_{0j}$  and the stress drop ( $\Delta\sigma$ ) are related through

$$f_{0j} = 4.9 \times 10^6 (N_{Rj})^{-1/3} N^{1/3} V_s \left( \frac{\Delta\sigma}{M_{0j}} \right)^{1/3} \quad (3)$$

Here  $V_s$  stands for the shear wave velocity in the source region, corresponding to bedrock conditions.  $N_{Rj}$  is the cumulative number of ruptured subfaults by the time rupture reaches the  $j^{\text{th}}$  subfault. The spatial modifying function  $D(f)$  is given by

$$D(r, f) = G \exp \left[ \frac{-\pi f r}{V_s Q(f)} \right] \quad (4)$$

where  $G$  is the geometric attenuation factor. The other term denotes anelastic attenuation with hypocentral distance  $r$  and the quality factor as  $Q$ . The spatial spread of the ground motion depends sensitively on the quality factor of the local region. The constant  $C$  of equation (4.1) is

$$C = \frac{\langle R_{\theta\phi} \rangle \sqrt{2}}{4\pi\rho V_s^3} \quad (5)$$

where  $\langle R_{\theta\phi} \rangle$  is the radiation coefficient averaged over an appropriate range of azimuths and take-off angles and  $\rho$  is the material density at the focal depth. The coefficient  $\sqrt{2}$  in the above equation arises as the product of the free surface amplification and partitioning of energy in orthogonal directions. The scaling factor for  $j^{\text{th}}$  sub-fault,  $H_j$  based on the squared acceleration spectrum is taken as (Boore 2009)

$$H_j = \sqrt{N} \frac{f_0^2}{f_{0j}^2} \quad (6)$$

Where  $f_0$  is the corner frequency at the end of the rupture, which can be obtained by substituting  $N_R(t) = N$  in equation (4.3). The filter function  $P_j(f)$  is taken as

$$P_j(f) = \frac{\sqrt{N}}{H_j} \frac{1 + (f/f_{0j})^2}{1 + (f/f_0)^2} \quad (7)$$

The moment of  $j^{\text{th}}$  subfault is computed from the slip distribution as follows

$$M_{0j} = \frac{M_0 D_j}{\sum_{j=1}^N D_j} \quad (8)$$

Here,  $D_j$  is the average final slip acting on the  $j^{\text{th}}$  subfault.  $M_0$  is the total seismic moment on the fault. To further account for earthquake rupture Motazedian and Atkinson (2005) introduced the concept of pulsing area where the cumulative number of active subfaults,  $N_{Rj}$  increases with time at the initiation of rupture and becomes constant at some fixed percentage of the total rupture area. This parameter determines the number of active subfaults during the rupture of  $j^{\text{th}}$  subfault. These many subfaults are used in computing the corner frequency in equation 3. The above is a general finite source model expressed in the frequency domain, valid for any region if only the various controlling parameters can be selected suitably. Here lies strength of this approach since almost all required parameters for India have been worked out in the past by geophysicists and seismologists using various types of instrumental data from small and large earthquakes. The parameters applicable at All India level are listed first. The spatial modifier of equation 4 consists of a general geometrical attenuation term  $G$ . This is taken following Singh *et al* (1999) as

$$G = \begin{cases} \frac{1}{r}, & \text{for } r \leq 100 \\ \frac{1}{10\sqrt{r}}, & \text{for } r > 100 \end{cases} \quad (9)$$

For in-slab events in northeast India, the geometrical attenuation term is taken as  $1/r^{1.55}$ . The shear wave velocity and density at the focal depth are fixed at 3.6 km/s and 2900 kg/m<sup>3</sup> respectively corresponding to compressed hard granite (Singh *et al* 2004).

#### 4. Regionalization in terms of geology

The effects that are specific to Indian geological regions appear in the quality factor  $Q(f)$ , stress drop value ( $\Delta\sigma$ ), focal depth, dip angle of the fault plane and the site amplification function  $F(f)$ . At this stage a brief discussion on the seismotectonic setting and geological structure of India to extract useful information for further work is necessary. Although, India can be broadly divided into Himalaya, Indo-Gangetic plain and peninsular Shield, the geology and earthquake activity is not uniform within the three regions. Due to the Indo-Burmese arc to the east and the syntaxis region, the northeastern India is more active compared to the rest of Himalaya. This region also contains Shillong plateau, fragmented part of the peninsular shield and the Bengal basin. In peninsular shield the Kutch region, Son Narmada region, west coast region are more active and exhibit different seismo-tectonics. The geology is also not uniform in Peninsular shield region. This demands dividing the three broad regions into further small zones for estimating seismic hazard. It appears from figure 1 and 3, shield can be further divided into three units namely Gujarat region, Central India and Peninsular India. The Gujarat region is defined to the west of the Marginal fault. The region to the south of Godavari river and comprising the Dharwar protocontinent is taken as the peninsular India. The central India lies in between peninsular India and the Gangetic plain and consists of Singhbhum and Aravali protocontinents. Northeast India which has complex geology and tectonics has to be treated separately for estimating hazard. This region is defined to the east of the Dhubri fault where the river Brahmaputra takes 90° turn. The Andaman region is treated as a separate tectonic unit. These regions are marked in Figure 2.

#### 5. Model Parameters

Among the model parameters, stress drop, focal depth, dip and quality factor will vary depending on the seismo-tectonic setup and geology of the region. Thus these five parameters have to be selected separately for all the seven regions in India. In the past several seismologists have analysed instrumental data to arrive at estimates of the frequency dependent quality factor, which is similar to the damping coefficient in elastic materials. On similar lines the value of stress drop

that can happen in different regions for a given magnitude of earthquake is available. Large amount of literature exists on the estimation of these parameters. The Quality factors available for all the seven regions are shown in Figure 2. The other important regional parameter is the focal depth which can vary from as low as 5 km to as deep as 100 km or deeper. The variation in focal depth is fairly well known for the different regions in India ( Kayal 2008). The range of focal depth, stress drop and dip in the seven regions are reported in Table 1. Apart from the above parameters, the S-wave radiation coefficient ( $\langle R_{\theta\phi} \rangle$ ) varies randomly within particular intervals. Here, following Boore and Boatwright (1984), the S-wave radiation coefficient is taken to be in the interval 0.48–0.64. In addition to the above parameters the slip distribution and pulsing percentage area is also required in the simulation. The pulsing percentage area is varied from 25% - 75% (Boore and Atkinson 2006). The stochastic finite fault approach requires slip distribution on the rupture plane which is highly complex. In this study the slip is simulated as a random field from the approach of Mai and Beroza (2002). The hypocenter in each case is taken nearer to the regions of maximum slip release. This sample slip field on the fault plane is discretized into subfaults of size 1 km x 1 km and seismic moment of each point source is computed using equation 8. Since the moment distribution on the rupture plane is modeled as random field, one can generate an ensemble of time histories at the surface by numerical simulation. To cover all possible peculiarities in the slip distribution, fifty samples of slip field are generated for each event.

The varying subsurface condition in the seven regions highlights the importance of selecting a common reference site for mapping seismic hazard. It remains to fix up the amplification function  $F(f)$  for A-type sites further work. The velocity structure from the basement to the surface can vary in a variety of ways. The A-type reference site can also be made of different layers of rocks making up the average value of  $V_{30} > 1.5$  km/s. Such sites are quite common in peninsular India and are also met with in Central and Northeast India. It can be observed that, since  $V_{30}$  is an average value, one can have several combinations of soil profiles leading to the same average value. Thus, in addition to uncertainties in seismological parameters, one has to consider the statistical variation in soil profiles for simulating representative surface level spectral accelerations. Here, a random sample of fifty profiles matching with A-type site categories is selected for further study. These are realistic as they are drawn from actual field investigations (Parvez *et al* 2002). Modification between bedrock and A-type site is a linear problem in one dimension and hence for such sites amplification can be directly found by the quarter-wavelength method of Boore and Joyner (1997).

## **6. Ground motion relations for A-type rock condition**

From the above discussion it is seen that once the stress drop, slip field, site amplification and  $Q$  factors are known, the Fourier amplitude spectrum of ground acceleration for any combination of magnitude ( $M_w$ ) and hypocentral distance ( $r$ ) can be expressed within the limitations of a finite source seismological source mechanism model. This is a random process and hence in the time domain this represents an ensemble of accelerograms. Here spectral acceleration values have been simulated for moment magnitude ( $M_w$ ) ranging from 4 to 8.5 in increments of 0.5 units, at 20 values of hypocentral distances ranging from 1 to 500 km. To capture finiteness of the source the ground motions are also simulated for eight azimuths ranging from  $0^\circ$  to  $315^\circ$  in increments of  $45^\circ$ . Thus a total number of 160 distance samples are considered for each magnitude. In all, there are 1600 pairs of magnitudes and distances. Since the stress drop, focal depth, dip, amplification function, radiation coefficient, pulsing percentage area are random variables and slip as a random field, we have included the uncertainty arising out of these parameters also. Accordingly, fifty samples of these seven seismic parameters are generated and these are combined using the Latin Hypercube sampling technique (Iman and Conover 1980) to select for each magnitude value fifty sets of random seismic parameters. Thus, a database of 80,000 PGA and  $S_a$  samples corresponding to 1600 simulated earthquake events are generated. This synthetic database is developed separately for each of the seven regions previously described using their respective quality factors. Among the seven regions peninsular India and northeast India need further area weighted refinement. This happens because the Koyna-Warna region and the remaining part of South India have different  $Q$ -factors. To account for this the simulated samples are individually simulated for each of the above sub-regions and combined in the ratio of 1:5 to assemble the final set of 80,000 samples for PI. Similarly the subduction zone and the shallow active zone in North East India are in the ratio 1:3 with differing  $Q$ -factors. Here also the samples have been generated separately and mixed together in the above ratio.

Several functional forms of ground motion attenuation have been proposed in the literature to reflecting salient aspects of the spread of ground motion (Sadigh *et al* 1997, Atkinson and Boore 2006). Since all the proposals are empirical the particular form selected are justified heuristically and sometimes by limited comparison with instrumental records. After reviewing the various available forms of equations, it has been decided to develop the attenuation relation for all the seven regions in the form

$$\ln\left(\frac{S_a}{g}\right) = c_1 + c_2 M + c_3 M^2 + c_4 r + c_5 \ln\left(r + c_6 e^{c_7 M}\right) + c_8 \log(r) f_0 + \ln(\varepsilon) \quad (10)$$

$$f_0 = \max(\ln(r/100), 0)$$

Here  $S_a$  is the spectral acceleration,  $M$  is the moment magnitude,  $r$  is the hypocentral distance in kilometers. This form of the attenuation accounts for geometrical spreading, anelastic attenuation and magnitude saturation similar to the finite source seismological model discussed previously. The coefficients of the above equation are obtained from the simulated database of 80,000 samples by regression analysis. The coefficients  $c_1, c_2, \dots, c_8$  and the standard error are shown in Tables 2a-b as functions of period (1/frequency) for peninsular India and Himalayan region.

The coefficients for other five regions have also been obtained. These results can be used to construct the mean and (mean+sigma) response spectrum on A-type rock in any part of peninsular India. In Figure 3 the attenuation of PGA in the all the seven regions is shown for different magnitude values. Figure 4 shows the response spectra for  $M_w$  6.5 event in all the seven regions at two hypocentral distances of 10km and 100km. Soil amplification has to be accounted for with the present attenuation relation for its implementation for the other types of soil condition.

As mentioned earlier the SMA data available for India is limited. Hence, it would be interesting to see how the derived synthetic attenuation relation matches with available observations. In Figures 5a-b the estimated PGA values for the Himalayan region are compared with recorded instrumental values of the Uttarkashi and Chamoli earthquake are shown. The present estimation are only expected values with considerable variation. Although the geotechnical details are not known, all the recording stations for these two events except Roorkee and Chinyalisur are located on granite, quartzite and sandstone (Chandrasekaran and Das 1992).

## 7. Summary and Conclusions

New ground motion relations for spectral acceleration have been developed for India in this paper. To derive these equations, India has been divided into seven regions based on seismo-tectonic setting and geology. In the absence of sufficient number of strong motion records, finite source seismological model is used to simulate samples of ground motion. The input parameters in the seismological model such as stress drop, depth of the fault, radiation coefficient, amplification function, pulsing percentage and dip are treated as random variables. The slip distribution is simulated as a random field. The variability of these model parameters in each region are taken from the literature. A synthetic database is simulated for all the seven geological zones in India. A total of 80,000 ground motion samples have been simulated from 1600 artificial earthquakes covering all ranges of magnitude and distances. These synthetic ground motion samples are further used to derive the empirical equations for India. The developed equations are valid for A-type rock sites in India. These equations can be used by engineers for obtaining the



design response spectrum. Ground motion prediction equations are generally used in assessing the probabilistic seismic hazard of a region or a specific site of interest. Many countries have come up with region specific ground motion relations which are used in PSHA and microzonation studies. The ground motion relations developed in this paper can be used to carry out the probabilistic seismic hazard assessment and to prepare microzonation maps for important urban agglomerations in India.

## ACKNOWLEDGMENTS

Thanks are due to Prof. R.N. Iyengar, Dr A.K. Shukla and Prof. M. L. Sharma for their help in demarcating the boundaries of the seven regions. The work reported here has been supported by the National Disaster Management Authority (NDMA), Government of India, under grant number CIE0910153NDMASTGR.

## REFERENCES

- Atkinson, G. M. and D. M. Boore (2006). Earthquake ground-motion prediction equations for eastern North America, *Bull. Seism. Soc. Am.* **96**, 2181--2205.
- Bodin, P. *et al.* (2004), Ground motion scaling in the Kachchh basin, India, deduced from aftershocks of the 2001 Mw 7.6 Bhuj earthquake, *Bulletin of the Seismological Society of America*, 94(5):1658-1669.
- Boore, D.M. (1983), Stochastic simulation of high - frequency ground motions based on seismological models of the radiated spectra, *Bull. Seism. Soc. Am.*, 73:1865 – 1894.
- Boore, D.M. (2009). Comparing stochastic point-source and finite-source ground motion simulations: SMSIM and EXSIM, *Bull. Seism. Soc. Am.* 99(6):3202-3216.
- Boore, D.M., and Joyner, W.B. (1997). Site amplifications for generic rock sites, *Bull. Seism. Soc. Am.*, 87(2):327-341.
- Brune, J.N. (1970), Tectonic stress and spectra of seismic shear waves from earthquakes, *Journal of Geophysical Research*, 75:4997 – 5009.
- Chandrasekaran, A.R. and Das, J.D. (1992), Strong motion arrays in India and analysis of data from Shillong array, *Current Sci.*, 62:233-250.
- Douglas, J. (2003), Earthquake ground motion estimation using strong-motion records: A review of equations for the estimation of peak ground acceleration and response spectral ordinates. *Earth-Science Reviews*, 61(1-2), 43–104.
- IBC. (2003). *International Building Code*. International Code Council.
- Iman, R.L. and Conover, W.J. (1980), Small sample sensitivity analysis techniques for computer models, with an application to risk assessment, *Communications in Statistics*, A9(17):1749-1842. Rejoinder to Comments, 1863-1874.

Iyengar, R.N. and Raghukanth, S.T.G. (2004), Attenuation of strong ground motion in peninsular India, *Seismological Research Letters*, 75(4), 530-540.

Kayal J.R. (2008), *Microearthquake Seismology and Seismotectonics of South Asia*. Capital Publishing Company, New Delhi.

Mai, P. M. and Beroza G. C. (2002) A spatial random field model to characterize complexity in earthquake slip. *J Geophys Res* 107:1–21.

Mohanty, W.K., Prakash, R., Suresh, G., Shukla, A.K., Walling, M.Y. and Srivastava, J.P. (2009), Estimation of coda wave attenuation for the national capital region, Delhi, India using local earthquakes, *Pure and Applied Geophysics*, 166(3): 429-449.

Motazedian, D., Atkinson, G. M. (2005) Stochastic finite fault modelling based on a dynamic corner frequency. *Bull. Seism. Soc. Am.*, 95(3):995–1010.

Parvez, I.A, Sutar, A.K, Mridula, M., Mishra, S.K. and Rai, S.S. (2008), Coda Q estimates in the Andaman Islands using local earthquakes, *Pure and Applied Geophysics*, 165:1861–1878.

Raghukanth S.T.G. and Somala S. N. (2009), Modeling of strong motion data in Northeastern India: Q, stress drop and site amplification, *Bull. seism. Soc. Am.*, 99(2A):705-725.

Raghukanth, S.T.G and Iyengar, R.N. (2007), Estimation of seismic spectral acceleration in Peninsular India, *Journal of Earth System Science*, 116(3):199 – 214.

Raghukanth S T G and Dash S K 2010 Deterministic seismic scenarios for northeast India *J. Seismol.* 14 143–67.

Rao, R., Seshamma, C.V. and Mandal, P. (1998). *Estimation of Coda  $Q_c$  and spectral characteristics of some moderate earthquakes of southern Indian peninsula*. Unpublished Report.

Sadigh, K., Chang, C. Y., Egan, J. A., Makdisi, F., and Youngs, R. R., (1997). Attenuation relationships for shallow crustal earthquakes based on California strong motion data, *Seismol. Res. Lett.* **68**, 180–189.

Sharma, B., Teotia, S.S. and Dinesh Kumar (2007), Attenuation of P, S, and coda waves in Koyna region, India, *Journal of Seismology*, 11:327–344.

Singh, S.K., Garc, D., Pacheco, J.F., Valenzuela, R., Bansal, B.K. and Dattatrayam, R.S. (2004), Q of the Indian Shield, *Bull. Seismol. Soc. Am.*, 94(4):1564-1570.

Table 1. Uncertainties in earthquake model parameters

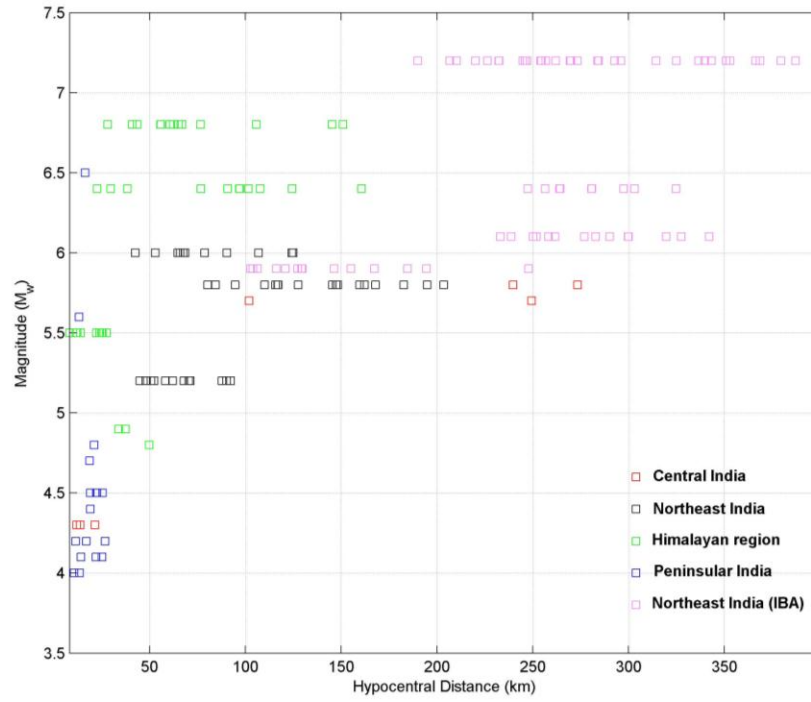
Region	Stress drop $\Delta\sigma$ (bars)	Dip ( $^{\circ}$ )	Focal depth (km)	Reference
Himalayas	50-200	2 <sup>0</sup> -30 <sup>0</sup>	5-40	Kayal (2008)
Northeast India-crustal	100-300	10 <sup>0</sup> -80 <sup>0</sup>	5-50	Kayal (2008)
Northeast India-Subduction	100-300	50 <sup>0</sup> -90 <sup>0</sup>	50-140	Kayal( 2008)
Indo-Gangetic plain	50-200	10 <sup>0</sup> -80 <sup>0</sup>	5-40	Kayal (2008)
Gujarat	100-300	10 <sup>0</sup> -80 <sup>0</sup>	5-40	Bodin <i>et al</i> (2004)
Central India	100-300	10 <sup>0</sup> -80 <sup>0</sup>	5-30	Singh <i>et al</i> (2004)
Andaman region	50-200	10 <sup>0</sup> -80 <sup>0</sup>	5-100	Parvez <i>et al</i> (2008)

Table 2a Coefficients in the attenuation relation for Peninsular India

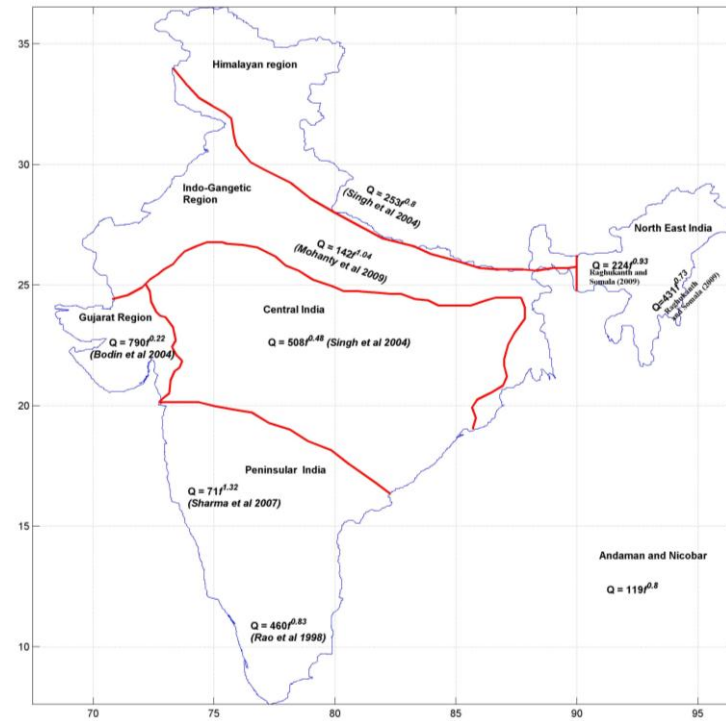
Period	C <sub>1</sub>	C <sub>2</sub>	C <sub>3</sub>	C <sub>4</sub>	C <sub>5</sub>	C <sub>6</sub>	C <sub>7</sub>	C <sub>8</sub>	$\sigma(\epsilon)$
0.0000	-5.2182	1.6543	-0.0309	-0.0029	-1.4428	0.0188	0.9968	0.1237	0.3843
0.0100	-5.2204	1.6523	-0.0307	-0.0029	-1.4422	0.0187	0.9971	0.1237	0.3837
0.0150	-4.1862	1.4952	-0.0197	-0.0030	-1.4265	0.0162	1.0135	0.1209	0.4159
0.0200	-4.1018	1.5037	-0.0209	-0.0030	-1.4096	0.0146	1.0237	0.1202	0.4022
0.0300	-4.1365	1.5228	-0.0227	-0.0030	-1.3888	0.0137	1.0298	0.1161	0.3873
0.0400	-4.2520	1.5430	-0.0244	-0.0029	-1.3783	0.0137	1.0266	0.1149	0.3827
0.0500	-4.4128	1.5817	-0.0271	-0.0029	-1.3801	0.0142	1.0227	0.1140	0.3822
0.0600	-4.7225	1.6531	-0.0327	-0.0028	-1.3730	0.0159	1.0077	0.1132	0.3835
0.0750	-5.0947	1.7235	-0.0383	-0.0028	-1.3572	0.0146	1.0136	0.1121	0.3842
0.0900	-5.5186	1.8218	-0.0460	-0.0028	-1.3441	0.0145	1.0117	0.1113	0.3856
0.1000	-5.8239	1.8911	-0.0511	-0.0028	-1.3409	0.0157	1.0018	0.1103	0.3868
0.1500	-7.4663	2.2950	-0.0816	-0.0027	-1.3179	0.0213	0.9581	0.1055	0.3888
0.2000	-9.0431	2.6930	-0.1115	-0.0026	-1.2965	0.0239	0.9374	0.1020	0.3941
0.3000	-11.9934	3.4705	-0.1687	-0.0025	-1.2861	0.0384	0.8713	0.0989	0.4008
0.4000	-14.3305	4.0665	-0.2112	-0.0025	-1.2686	0.0462	0.8467	0.0984	0.4052
0.5000	-16.2504	4.5566	-0.2457	-0.0024	-1.2614	0.0533	0.8254	0.0975	0.4082
0.6000	-18.1350	5.0060	-0.2767	-0.0024	-1.2419	0.0473	0.8363	0.0949	0.4106
0.7000	-19.3494	5.3013	-0.2962	-0.0024	-1.2399	0.0508	0.8309	0.0934	0.4119
0.7500	-19.8904	5.4156	-0.3035	-0.0023	-1.2316	0.0472	0.8388	0.0922	0.4130
0.8000	-20.4426	5.5522	-0.3118	-0.0023	-1.2423	0.0529	0.8273	0.0938	0.4120
0.9000	-21.4875	5.7648	-0.3246	-0.0023	-1.2309	0.0473	0.8383	0.0922	0.4129
1.0000	-21.9767	5.8581	-0.3297	-0.0023	-1.2258	0.0438	0.8487	0.0927	0.4134
1.2000	-23.1660	6.0486	-0.3372	-0.0023	-1.2204	0.0401	0.8659	0.0939	0.4139
1.5000	-24.2031	6.1891	-0.3402	-0.0022	-1.2281	0.0371	0.8833	0.0924	0.4137
2.0000	-25.1523	6.2202	-0.3308	-0.0022	-1.2390	0.0324	0.9107	0.0975	0.4173
2.5000	-25.5577	6.1153	-0.3139	-0.0022	-1.2275	0.0213	0.9687	0.0982	0.4248
3.0000	-25.5807	5.8957	-0.2871	-0.0021	-1.2341	0.0150	1.0215	0.1003	0.4274
4.0000	-25.2671	5.5029	-0.2436	-0.0021	-1.2511	0.0122	1.0627	0.1034	0.4346

Table 2b. Coefficients in the attenuation relation for Himalayan region

Period	C <sub>1</sub>	C <sub>2</sub>	C <sub>3</sub>	C <sub>4</sub>	C <sub>5</sub>	C <sub>6</sub>	C <sub>7</sub>	C <sub>8</sub>	$\sigma(\epsilon)$
0.0000	-3.7438	1.0892	0.0098	-0.0046	-1.4817	0.0124	0.9950	0.1249	0.4094
0.0100	-3.7486	1.0877	0.0099	-0.0046	-1.4804	0.0123	0.9955	0.1247	0.4083
0.0150	-2.7616	0.9550	0.0188	-0.0049	-1.4649	0.0111	1.0051	0.1234	0.4678
0.0200	-2.7051	0.9588	0.0179	-0.0049	-1.4387	0.0092	1.0246	0.1223	0.4445
0.0300	-2.7582	0.9755	0.0162	-0.0048	-1.4121	0.0081	1.0372	0.1179	0.4137
0.0400	-2.9321	1.0173	0.0126	-0.0047	-1.4014	0.0087	1.0248	0.1165	0.4001
0.0500	-3.0839	1.0461	0.0106	-0.0046	-1.3992	0.0089	1.0217	0.1124	0.3941
0.0600	-3.3069	1.0905	0.0075	-0.0046	-1.3958	0.0095	1.0129	0.1150	0.3910
0.0750	-3.6744	1.1532	0.0024	-0.0046	-1.3738	0.0086	1.0202	0.1145	0.3885
0.0900	-4.1011	1.2448	-0.0045	-0.0046	-1.3582	0.0086	1.0173	0.1146	0.3873
0.1000	-4.4163	1.3088	-0.0092	-0.0045	-1.3480	0.0089	1.0131	0.1095	0.3873
0.1500	-5.8898	1.6365	-0.0331	-0.0043	-1.3168	0.0101	0.9903	0.1011	0.3882
0.2000	-7.3244	1.9682	-0.0572	-0.0043	-1.2859	0.0096	0.9891	0.0987	0.3929
0.3000	-9.9600	2.6152	-0.1031	-0.0040	-1.2659	0.0134	0.9404	0.0926	0.4010
0.4000	12.1052	3.1363	-0.1391	-0.0040	-1.2445	0.0166	0.9136	0.0878	0.4060
0.5000	-13.8894	3.5767	-0.1691	-0.0039	-1.2403	0.0188	0.8940	0.0906	0.4069
0.6000	-15.6887	3.9957	-0.1974	-0.0038	-1.2192	0.0181	0.8930	0.0876	0.4085
0.7000	-16.8075	4.2512	-0.2137	-0.0038	-1.2118	0.0187	0.8939	0.0863	0.4078
0.7500	-17.3641	4.3748	-0.2219	-0.0038	-1.2038	0.0183	0.8934	0.0842	0.4096
0.8000	-17.9297	4.5173	-0.2306	-0.0037	-1.2175	0.0221	0.8745	0.0847	0.4070
0.9000	-19.0065	4.7521	-0.2452	-0.0037	-1.2109	0.0231	0.8670	0.0861	0.4072
1.0000	-19.5191	4.8564	-0.2515	-0.0037	-1.2044	0.0224	0.8699	0.0854	0.4081
1.2000	-20.8567	5.1139	-0.2652	-0.0036	-1.2027	0.0236	0.8720	0.0868	0.4007
1.5000	-22.0907	5.3398	-0.2751	-0.0035	-1.2231	0.0254	0.8731	0.0871	0.3958
2.0000	-23.4263	5.5337	-0.2796	-0.0034	-1.2496	0.0283	0.8733	0.0946	0.3898
2.5000	-24.1315	5.5606	-0.2742	-0.0033	-1.2525	0.0245	0.8965	0.0971	0.3924
3.0000	-24.6217	5.5327	-0.2635	-0.0032	-1.2779	0.0238	0.9092	0.1009	0.3951
4.0000	-24.8660	5.3573	-0.2394	-0.0031	-1.3022	0.0224	0.9280	0.1076	0.4023



**Figure 1. Available instrumental database in India**



**Figure 2. Seven geological provinces with differing quality factors**

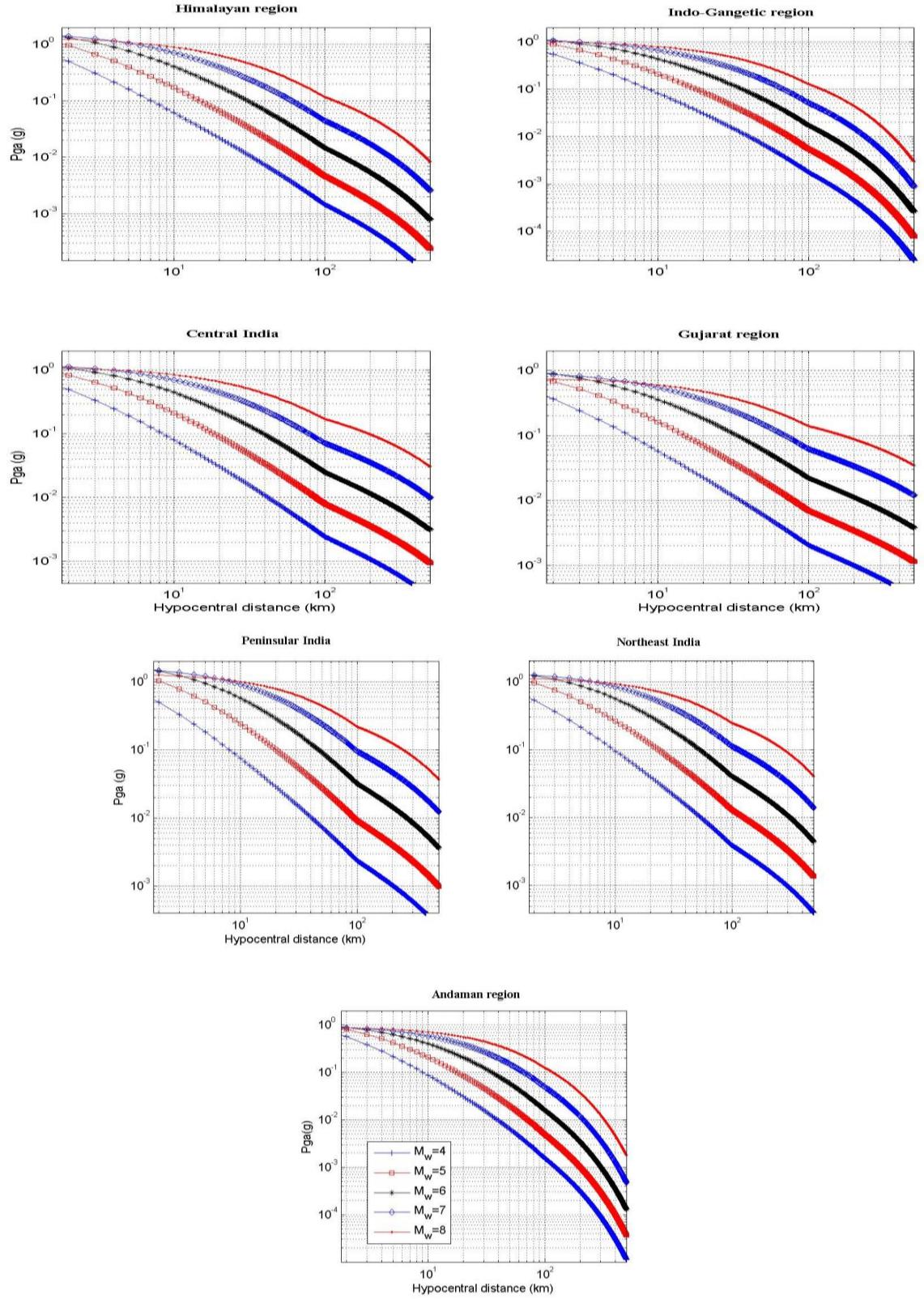
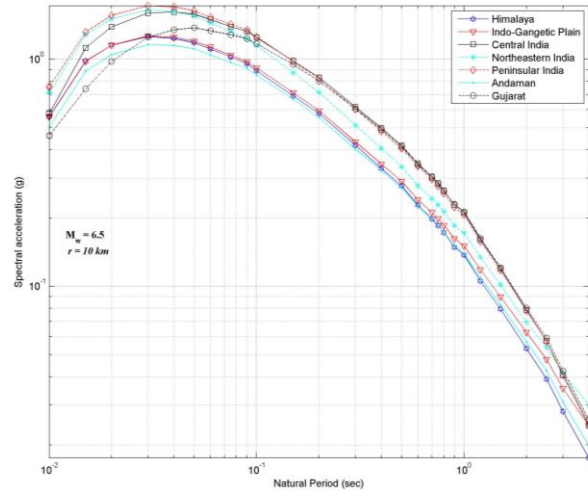
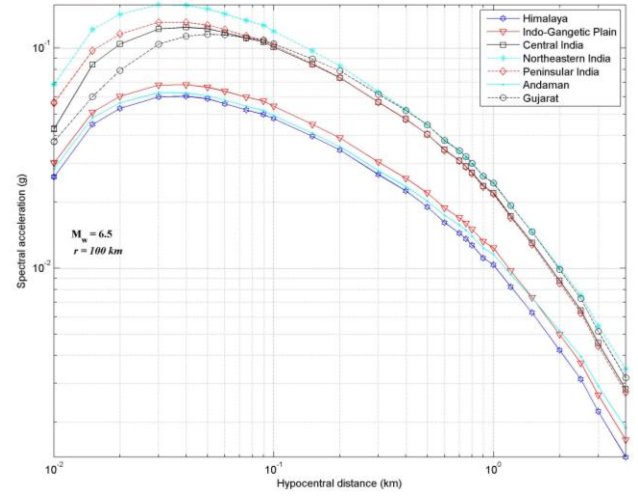


**Figure 3. Attenuation of ZPA (in g) with hypocentral distance at Type A rock level for different regions of India**

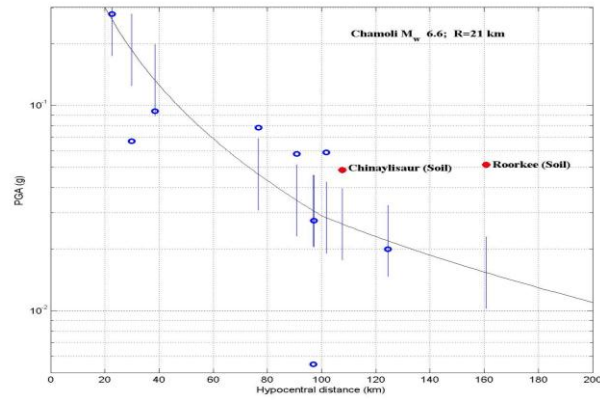


a)

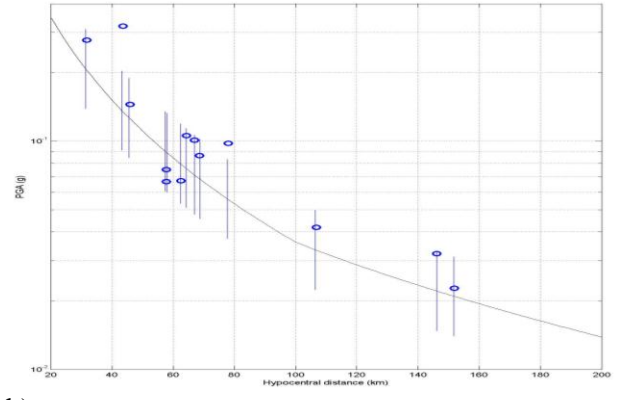


b)

**Figure 4. Response spectra for the seven sub-regions in India of figure 2**



a)



b)

**Figure 5. Attenuation in the Himalayan region. a) PGA data of Chamoli earthquake 29<sup>th</sup> October 1999 ( $M_w$  6.6). b) PGA data of Uttarkashi earthquake 20<sup>th</sup> October 1991 ( $M_w$  6.8) . Vertical bands indicate 1-sigma width about the mean value.**